

former is still a very potent drug; however, because of a scarcity of sample, didemnin A has not yet been evaluated at optimum dosage levels for its antitumor effect in vivo. Didemnin C, the trace component, has not been available in quantities adequate for extensive testing.

Interest in the chemotherapeutic potential of the didemnins is heightened by recent investigations (9) resulting in the structure elucidation of didemnins A, B, and C (Fig. 1). Novel aspects are a new structural unit for depsipeptides, hydroxyisovalerylpropionate, and a new stereoisomer of the highly unusual amino acid statine. It is particularly noteworthy that didemnins B and C are simple derivatives of didemnin A. That the biological activities of the didemnins can be dramatically altered by slight chemical changes bodes well for the development of a useful therapeutic agent.

KENNETH L. RINEHART, JR.
JAMES B. GLOER

Roger Adams Laboratory,
University of Illinois, Urbana 61801

ROBERT G. HUGHES, JR.
Department of Cell and Tumor Biology,
Roswell Park Memorial Institute,
Buffalo, New York 14263

HAROLD E. RENIS
J. PATRICK MCGOVREN
EVERETT B. SWYNENBERG
DALE A. STRINGFELLOW
SANDRA L. KUENTZEL
LI H. LI

Upjohn Company,
Kalamazoo, Michigan 49001

References and Notes

1. Presented in part at the 3rd International Symposium on Marine Natural Products (International Union of Pure and Applied Chemistry and Société Chimique de Belgique), Brussels, 16 September 1980.
2. P. D. Shaw, W. O. McClure, G. Van Blaricom, J. Sims, W. Fenical, J. Rude, in *Food-Drugs from the Sea Proceedings 1974*, H. H. Webber and G. D. Ruggieri, Eds. (Marine Technology Society, Washington, D.C., 1976), pp. 429-433; K. L. Rinehart, Jr., R. D. Johnson, I. C. Paul, J. A. McMillan, J. F. Siuda, G. E. Krejcarek, *ibid.*, pp. 434-442.
3. K. L. Rinehart, Jr., *et al.*, *Pure Appl. Chem.* **53**, 795 (1981).
4. M. T. Cheng and K. L. Rinehart, Jr., *J. Am. Chem. Soc.* **100**, 7409 (1978).
5. G. T. Carter and K. L. Rinehart, Jr., *ibid.*, p. 7441.
6. By Dr. Françoise Lafargue, Laboratoire Arago, Banyuls-sur-mer, France, and Dr. Charles C. Lambert, Department of Biological Science, California State University, Fullerton.
7. H. E. Renis, *Antimicrob. Ag. Chemother.* **11**, 701 (1977); *ibid.* **13**, 613 (1978).
8. ———, unpublished data.
9. K. L. Rinehart, Jr., J. B. Gloer, J. C. Cook, Jr., S. A. Mizsak, and T. Scahill, *J. Am. Chem. Soc.* **103**, 1857 (1981).
10. Supported in part by grants from the National Institute of Allergy and Infectious Diseases (AI 04769), the National Institute of General Medical Sciences (GM 27029), and from the National Science Foundation (PCM 77-12584). We thank the governments of Colombia, Honduras, Mexico, Belize, and Panama for permission to carry out scientific research in their territorial waters.

22 September 1980; revised 6 February 1981

Gated Sodium-23 Nuclear Magnetic Resonance Images of an Isolated Perfused Working Rat Heart

Abstract. Sodium-23 nuclear magnetic resonance images of phantoms and gated images of isolated perfused working rat hearts were obtained. By synchronizing the nuclear magnetic resonance process to the heartbeat, images were obtained at systole and at diastole.

Since its inception (1), nuclear magnetic resonance (NMR) imaging has progressed from a curiosity to the point where it promises to become one of the more important diagnostic tools in medicine. Several examples of high-resolution (millimeter) NMR images of protruding appendages of the human body, notably limbs and heads, have been published (2-4). Technological progress is being made, and NMR images of cross sections of the human torso may soon have a resolution comparable to that now obtained for heads and limbs. It is important that methods for using NMR imaging as a noninvasive diagnostic modality in cardiovascular research be developed.

Gating the acquisition of NMR signals to the heartbeat (5) was essential in our experiment in order to overcome the problems posed by heart motion. In addition to developing NMR technology suitable for imaging a beating heart, the physiological basis for providing contrast between the heart and the blood must be identified. Proton NMR images based on proton density alone may provide little contrast between blood and surrounding tissues. However, there is a significant difference between the concentration of sodium in blood and that in healthy tissue. We sought, therefore, to produce ²³Na NMR images of the heart. They would be negative images of the myocardium inasmuch as healthy tissue has a low sodium content compared to blood.

For these experiments, we modified a Nicolet wide-bore NT 360 spectrometer (8.45 T) so that it would perform as an imaging instrument. This involved the addition of three computer-controlled digital-to-analog converters to vary the currents of the first-order gradient shim coils, and the composition of several routines to provide these controls during acquisition of NMR data and to allow reconstruction and display of images. The imaging method used was basically the projection reconstruction method (1) with the image plane defined by an adaptation of the z-gradient oscillation method. The thickness of the slice was established experimentally by use of a phantom consisting of a flat-bottom NMR

tube with a thin layer (1 mm) of 100 mM NaCl on the bottom. By moving this phantom in the probe with the oscillating z gradient on, the thickness of the imaged slice was found to be about 1.5 mm. The acquisition of each free-induction decay was triggered from the aortic pressure wave. A delay between the trigger from the pressure wave and acquisition is programmed in order to choose the instant within the cardiac cycle at which the acquisition is triggered.

As has traditionally been the case, the image-producing system was validated by making ²³Na images of phantoms. Figure 1a shows a diagram of the cross section of a phantom that consisted of a 20-mm outer diameter NMR tube filled with distilled water, into which were placed 5- and 2-mm outer diameter tubes containing 145 mM NaCl. Figure 1b is the ²³Na NMR image of this phantom (obtained at 95.25 MHz) resulting from 12 projections in the x-y plane and reconstructed by the standard back-projection method. Each projection required averaging of 320 free-induction decays. The images shown in this report are defined by a matrix of 64 by 64 pixels and were photographed from the screen of a Hewlett-Packard 1304A, producing (unfortunately) minimal levels of contrast.

We obtained images of an isolated perfused working rat heart, using the perfusion apparatus previously described (5). The only modification was that the suction cannula was raised so that the level of perfusate in the NMR tube was above the heart. Since the perfusate (modified Krebs-Henseleit bicarbonate, pH 7.24) has a high sodium content, its presence external to the heart provided contrast to the ventricular wall. Gated planar images were obtained of a midventricular slice of the isolated working heart of a 350-g Sprague-Dawley rat (Fig. 2). These images were reconstructed from 12 projections, each projection obtained by averaging 320 free-induction decays. Since the spin-lattice relaxation time of sodium is short (approximately 40 msec) in tissue, acquisitions can be closely spaced. One free-induction decay can be collected during each heartbeat (approximately 230 msec). Thus each image required

about 15 minutes of data acquisition. In order to test the planar selectivity, a plane 5 mm lower (that is, at the apex) was imaged exactly as was the midventricular plane. Figure 3a shows a schematic representation of the sample at this level. The images are shown in Fig. 3, b and c.

Comparison of b and c of Fig. 2 shows an increase in wall thickness in systole

and an increase in cross-sectional area of the ventricular cavity in diastole. In the isolated working heart preparation, the right ventricle does not fill and therefore is not observable. As expected, the images in Fig. 3 are not different from each other, since the image plane was below the bottom of the cavity. In order to calculate ejection fraction, we assumed that the rat left ventricular cavity could

be represented by a prolate ellipse and that the major axis was twice as long as the minor axis (6). On the basis of these assumptions we calculated an ejection fraction of 56 percent, using standard formulas developed for human echocardiography. Imaging in three dimensions or imaging multiple slices may in the future allow for measurement of actual ejection fraction without resorting to the assumptions above. Other indicators of left ventricular function such as left ventricular mass, rate of circumferential shortening, and fractional shortening could also be calculated.

The NMR images in this report were obtained on a commercially available high-resolution NMR spectrometer designed according to criteria quite different from those that would be optimum for an NMR imaging instrument. In particular, the gradient coils were not modified and the radio-frequency coils were a Helmholtz saddle-shaped pair. This caused the edge distortions which are evident in the images in Figs. 2 and 3. Although these images contain imperfections, they do demonstrate several things. First, they show that ^{23}Na can be used as an alternative to (and perhaps an improvement on) protons for obtaining important physiological information such as the ejection fraction. Second, they show that gating the NMR imaging process to the cardiac cycle, much as is done in nuclear medicine and ultrasound, can solve the problem of imaging a moving organ by NMR.

JEAN L. DELAYRE

Department of Physiology and
Biophysics, Harvard Medical School,
Boston, Massachusetts 02115

JOANNE S. INGWALL

CRAIG MALLOY

Department of Medicine,
Harvard Medical School, and
Department of Medicine,
Brigham and Women's Hospital,
Boston, Massachusetts 02115

ERIC T. FOSSEL

Department of Physiology and
Biophysics, Harvard Medical School

References and Notes

1. P. C. Lauterbur, *Nature (London)*, **242**, 190 (1973).
2. W. S. Hinshaw, P. A. Bottomley, G. N. Holland, *ibid.*, **270**, 722 (1977).
3. G. N. Holland, R. C. Hawkes, W. S. Moore, *J. Comput. Assist. Tomography* **4**, 429 (1980).
4. _____, *ibid.*, p. 577.
5. E. T. Fossel, H. E. Morgan, J. S. Ingwall, *Proc. Natl. Acad. Sci. U.S.A.* **77**, 3654 (1980).
6. H. Feigenbaum, *Echocardiography* (Lea & Febiger, Philadelphia, 1976), pp. 317-320.
7. This work was completed during the tenure of J.S.I. and E.T.F. as established investigators of the American Heart Association and was supported by grants HL 22542 and HL 26215 from the National Institutes of Health.

22 December 1980

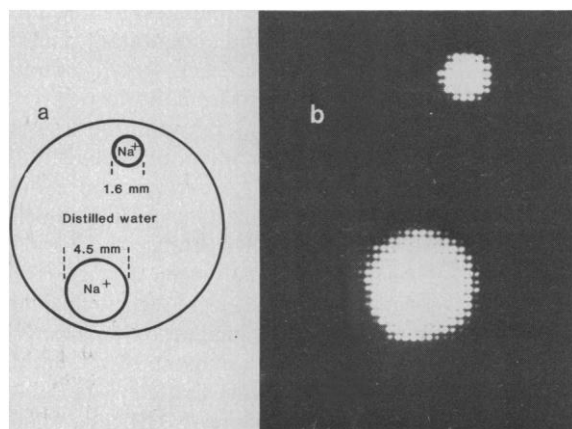


Fig. 1. (a) Diagrammatic representation of a phantom consisting of a 5- and a 2-mm outer diameter NMR tube, both containing 145 mM NaCl. The tubes were placed in a 20-mm outer diameter NMR tube containing distilled water. (b) Sodium-23 NMR image of the phantom shown in (a).

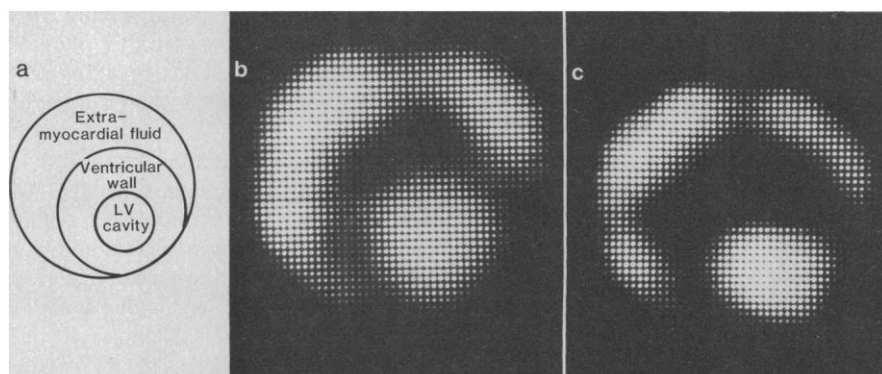


Fig. 2. (a) Diagrammatic representation at the midventricular level of an isolated perfused heart in the NMR sample tube. (b) Gated ^{23}Na NMR image of an isolated perfused working rat heart in diastole. The image plane is at the midventricular level. The heart is off center in the sample tube with the wall of the right ventricle in contact with the wall of the sample tube. (c) An equivalent image at systole.

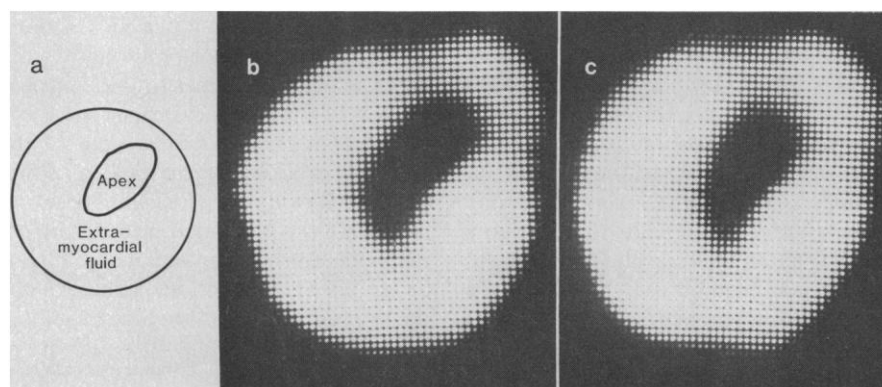


Fig. 3. (a) Diagrammatic representation at the apex of an isolated perfused heart in the NMR sample tube. (b) Gated ^{23}Na NMR image of an isolated perfused working rat heart in diastole. The image plane is near the apex. (c) An equivalent image at systole.